5th SASTech
Iran |Mashhad
May 12 - 17 | 2011
5th Symposium on Advances in Science & Technology

Comparative Study Of Current Control Schemes For Grid-Connected Photovoltaic Systems

Mojtaba Saleh, Electrical Engineering Dept.Iran University of Science and Technology
m_saleh@elec.iust.ac.ir
Prof. Abbas Shoulaie, Electrical Engineering Dept. Iran University of Science and Technology, Shoulaie@iust.ac.ir

Paper Reference Number:
Name of the Presenter: Mojtaba Saleh

Abstract

This paper presents three current control (CC) scheme for a three phase grid connected to photovoltaic (PV) system. In this work, complete PV system with different CC schemes have been simulated in MATLAB/SIMULINK and Comparison between presented schemes has been made in terms of dynamics performance, maximum power point tracking (MPPT), injected current quality and required number of switching.

Key words: Grid Connected Inverter; Current Control Scheme; PV Systems,;Renewable Energies.

1. Introduction

The excessive problem of greenhouse gases emissions worldwide and global energy crises has prompted interest in the issue of renewable energy sources. Among all renewable energy sources, photovoltaic energy is more attractive due to its great abundance and falling trend in cost of PV-cells. The grid connection of PV systems is a fast growing area, with a vast potential for domestic and industrial locations. A grid-connected PV system provides power supply for both the an individuals and industries or business with the means to be their own power producer, as well as contributing to an environmentally friendly agenda.

A simple block diagram of a grid connected PV system is shown in Fig. 1. The inverter's controller adjusts injected line current in a same level and maintains power balance between DC-DC converter and inverter so that voltage of DC-link is fixed in a constant value.

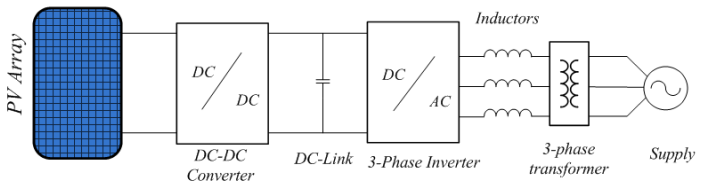

Fig. 1 Block diagram of a typical grid connected PV system.

The characteristic of a PV-cell is shown in Fig. 2. Due to nonlinear characteristic of PV arrays that varies with temperature and irradiance, a DC-DC converter must be used.

Its main task is to move operational point of PV-array toward maximum power point (MPP).

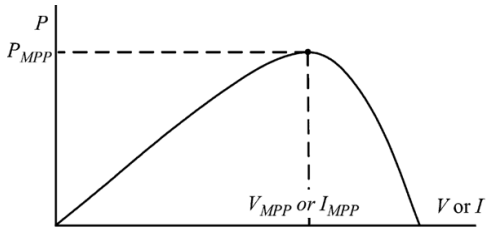

Fig. 2 Electrical characteristic of typical PV- cell.

The inverter needs a voltage larger than PV-array's voltage, on DC-link, therefore DC-DC converter acts as a boost converter. In this paper simple boost converter is used.
Simulation results will be presented to give a better view in comparison of three current control scheme of inverter.

2. MPPT Controller

There is several MPPT scheme specially designed to work with grid-connected PV systems [1-2]. Although other schemes such as perturb and observe (P&O), hill climbing and incremental conductance (IC) are applicable for these systems [3]. The duty cycle of ideal boost converter is given by :

$$d = 1 - V_{pv} / V_{dc} \quad (1)$$

Where V_{pv} and V_{dc} are voltage across PV-array and DC-link, respectively. If grid connected inverter controlled in such a way that V_{dc} kept constant, increment in d will result in decrement of V_{pv} and Vice Versa. Reference [3] made a good comparison between MPPT methods that (IC) method has been shown to has good performance and acceptable simplicity in implementation. Therefore IC algorithm will be described in follows and used in simulations. Basis of IC method is shown in Table 1.

Table 1 Basis of IC methode.

at MPP	$dP/dV = 0$	$\Delta V/\Delta I = -V/I$
left of MPP	$dP/dV < 0$	$\Delta V/\Delta I < -V/I$
right of MPP	$dP/dV > 0$	$\Delta V/\Delta I > -V/I$

Therefore MPP can be tracked by comparing instantaneous conductance (V/I) and incremental conductance (ΔV/ΔI).
IC method is generally used with fixed step size. Large step size contributes to fast dynamics but large oscillation around MPP which results in a relatively low efficiency. Small step size reverses this situation . So using IC method with variable step size proportional to $|\Delta P/\Delta V|$ is employed herein to solve this issue [4]. Update rule for boost converter duty cycle can be obtained as follows:

$$D(k) = D(k-1) \pm \Delta D = D(k-1) \pm C \times |\Delta P/\Delta V| \quad (2)$$

Where coefficient C is the scaling factor which is manually tuned at the design time to adjust the step size . Flow chart for IC MPPT with variable step size algorithm is shown in Fig. 3.

3. Current Control Methods in Grid-Connected Inverters

A voltage source inverter (VSI) in a grid-connected PV system as a interface between DC/DC power conversion and AC grid must be controlled in such a way that satisfies some criteria:

- inject sinusoidal current with low total harmonic distortion (THD) into grid with unity power factor.
- maintain power balance in order to fix dc-link voltage at a certain level.
- ensure good dynamics as environmental conditions changing

Therefore a current control scheme is employed that its main task is to generate switching states to force the current with appropriate waveform to the grid. So many control schemes have been proposed in the literature. Proposed concepts cover a wide variety from simple to quite complicated. In complicated cases some intelligent methods such as neural networks (NN's) and fuzzy logic controllers (FLC's) [5] have been used. In this paper just three simple and traditional current control scheme will be presented.

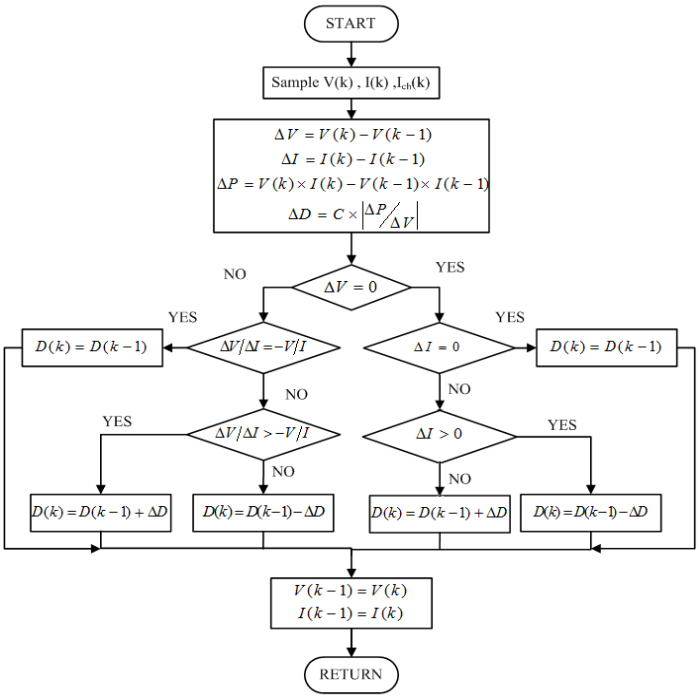

Fig. 3 Flowchart Of Variable Step Size IC MPPT Algorithm.

3.1. Hysteresis Current Control

The block diagram of grid-connected PV system with hysteresis current control at output current of voltage source inverter (VSI) is shown in Fig. 5. DC-link voltage ,V_{dc} , measured and compared with reference value and the error used to generate reference for output currents via PI compensator [6]. Output currents of inverter, i_a , i_b, i_c, measured and compared with reference values, i_a^*, i_b^*, i_c^*, and generated current errors and current controllers generate switching states ,a , b and c. The characteristic of current controller for phase A , $a = f(\Delta i_A)$, is shown in Fig. 4.

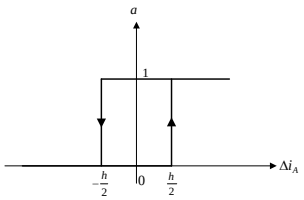

Fig. 4 Hysteresis current controller characteristic.

$$a=\begin{cases}0 & \Delta i_A < -h/2\\ 1 & \Delta i_A > h/2\end{cases} \quad (3)$$

Where *h* is hysteresis width that determines the acceptable current error. If output current error exceeds *h/2*, *a* will give value of 1 and SW_1 will be turn on and makes v_A positive and increases output current. If current error becomes lower than *–h/2*, signal a will give value of 0 and SW_2 will be turn on and makes v_A negative and decreases output current. It's also the same for phases b and c. Schematic diagram of hysteresis current control for grid connected PV system is shown in Fig. 5.

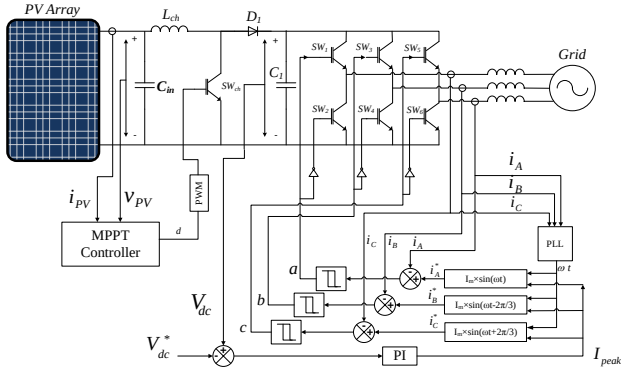

Fig. 5 schematic of hysteresis current control for a grid connected PV system .

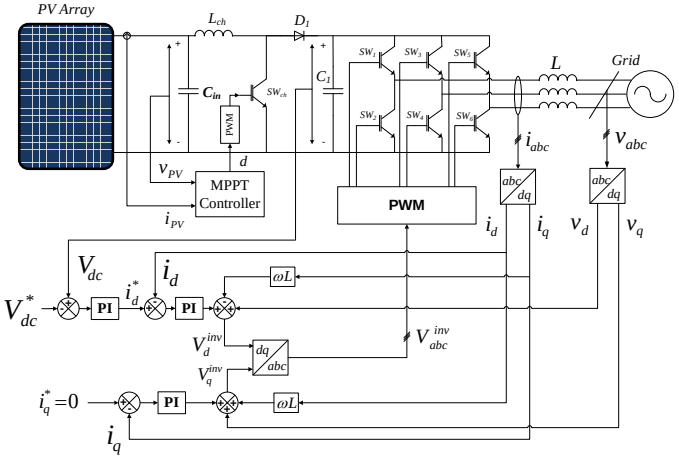

Fig. 6 schematic of linear current control for a grid connected PV system .

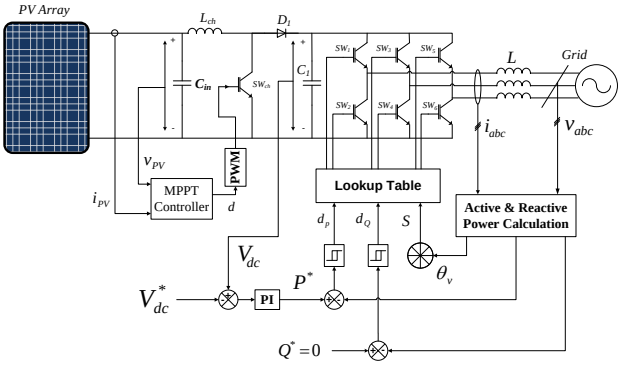

Fig. 7 Schematic of DPC current control for a grid connected PV system .

3.2. Linear Current Control

In this method output currents measured and mapped into rotating synchronous coordinates dq. Thanks to the coordinate transformations, i_d and i_q are dc components, and PI compensators reduce the errors of the fundamental component to zero [6]. The schematic of linear current control for a grid connected PV system is shown in Fig. 6. The voltage equation of source side of inverter are as follow :

$$[v_a^{inv} \quad v_b^{inv} \quad v_c^{inv}]^T = L\frac{d}{dt}[i_a \quad i_b \quad i_c]^T + R[i_a \quad i_b \quad i_c]^T + [v_a \quad v_b \quad v_c]^T \tag{4}$$

This equation may be translated into dq synchronous coordinates that may be aligned to axis d voltage ($v_q = 0$, $v_d = v_{inv}$):

$$v_d^{inv} = Ri_d + L\frac{d}{dt}i_d - \omega Li_q + v_d \quad , \quad v_q^{inv} = Ri_q + L\frac{d}{dt}i_q + \omega Li_d + v_q \tag{5}$$

Where ω the speed of the reference system or the supply frequency . The voltage decoupler is needed in order to have a independent control over d-q components:

$$v_d'^{inv} = \omega Li_q + v_d \quad , \quad v_q'^{inv} = -\omega Li_d \tag{6}$$

As shown in Fig. 6 voltage decoupler components are also taken into consideration. The injected reactive power is usually set to zero (i_q^*=0). The DC-link voltage is kept constant to take advantage of full voltage for capacitor energy, therefore apart from DC currents (i_q , i_d) controller, there is also controller loop for V_{dc}.

3.3. Direct Power Control (DPC)

This method is on the basis of instantaneous active and reactive power error and position of supply voltage space vector, the most suitable switching states are selected from switching table (ST) for next sampling period [7]. The schematic of DPC current control for a grid connected PV system is shown in Fig. 7. The output voltage of inverter at AC side in respect to DC-link voltage, V_{dc} , in dq synchronous coordinates are as follows :

$$\begin{aligned} v_d^{inv} &= \left[\frac{1}{\sqrt{6}}(2S_a - S_b - S_c)\cos\omega t + \frac{1}{\sqrt{2}}(S_b + S_c)\sin\omega t\right]V_{dc} \\ v_q^{inv} &= \left[\frac{1}{\sqrt{2}}(S_b - S_c)\cos\omega t - \frac{1}{\sqrt{6}}(2S_a - S_b - S_c)\sin\omega t\right]V_{dc} \end{aligned} \tag{7}$$

Each switching state result in a sinusoidal waveform for v_d^{inv} and v_q^{inv} as shown in Fig. 8. As shown in Fig. 7 DC-link voltage error is used to generate active power reference and in order to achieve unity power factor reactive power reference is set to zero. Active and reactive powers are calculated by using measured voltages and currents, and power errors delivered to hysteresis controllers. Controllers' output and supply voltage vector position are used to select a suitable switching state according to switching table (ST). Each switching state applied, causes a change in active and reactive powers. Active and reactive powers in dq synchronous coordinates are as follows :

$$P = v_d i_d + v_q i_q \quad , \quad Q = v_q i_d - v_d i_q \tag{8}$$

In case of balance supply voltage $v_q=0$ and $v_d = \sqrt{3/2}v_m$.

By neglecting $L\omega i_q$ and $L\omega i_d$ terms from equations (5), we can express the rate of active and reactive power changes as follows:

$$\frac{dP}{dt} \propto \sqrt{\frac{3}{2}}v_m - v_d^{inv} \quad , \quad \frac{dQ}{dt} \propto v_q^{inv} \tag{9}$$

Where v_m is the amplitude of supply line voltage. According to Fig. 8, in order to control active and reactive power, suitable switching state should be chosen to make right side of (9) positive or negative.

The ST used in this paper, at first have been proposed in [7] proposed and afterward improved in [8]. This ST presented in Table 2 and corresponding plane of voltage vector is shown in Fig. 9.

Table 2 Switching table for the improved DPC scheme.

dp	dq	sector											
		1	2	3	4	5	6	7	8	9	10	11	12
1	0	101	101	100	100	110	110	010	010	011	11	001	001
	1	111	000	000	111	111	000	000	111	111	000	000	111
0	0	100	100	110	110	010	010	011	011	001	001	101	101
	1	110	110	010	010	011	011	001	001	101	101	100	100

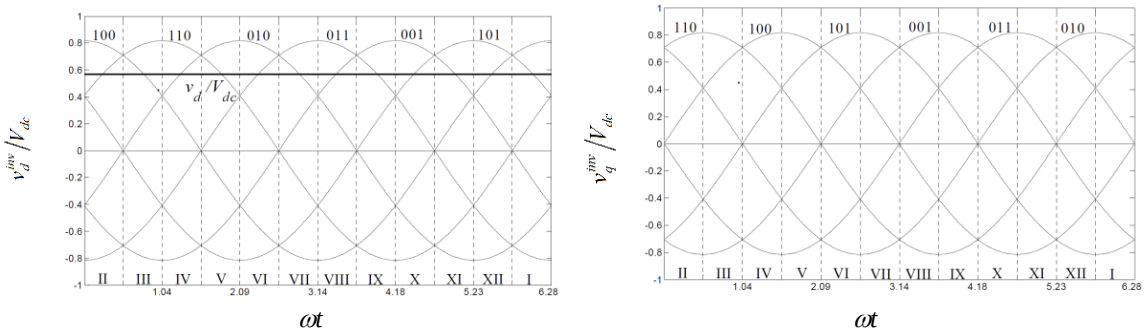

Fig. 8 v_d^{inv} and v_q^{inv} in each switching state.

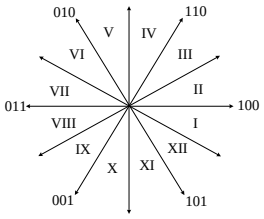

Fig. 9 Twelve sectors of the voltage plane used in DPC.

4. Simulation Results

Simulation is carried out to evaluate performance of grid-connected PV system under different control schemes for grid connected inverter. At first based on parameters given in **Error! Reference source not found.** for 36-cell 60 Watt OFFC PV module, a suitable model [9] developed in MATLAB/SIMULINK® for a PV-array consist of 5 module connected in parallel. Then complete system simulated with different control schemes. The simulation results under variable environmental conditions will be presented.

The variation of environmental conditions through time is shown in Fig. 10. As environmental conditions variation, the PV-array characteristics and MPP vary and MPPT controller, by making change in duty cycle of DC-DC converter, set operation point at MPP. Fig. 12 gives a comparative view on quality of injected current.

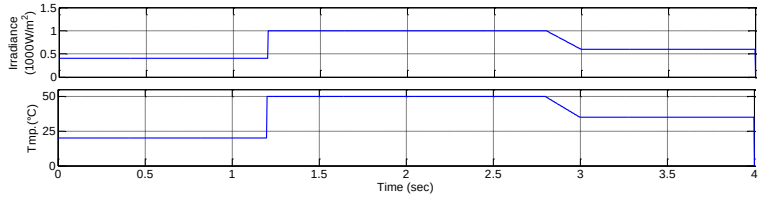

Fig. 10 Variation of Temperature and Irradiance.

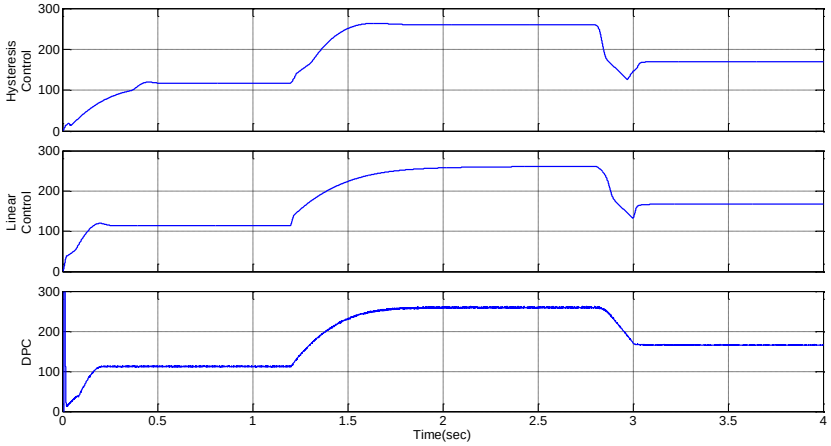

Fig. 11 Injected power by inverter for different CC schemes.

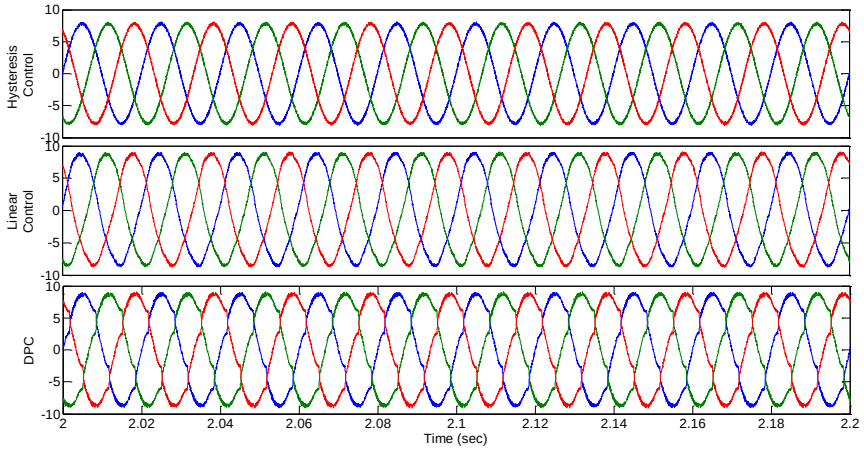

Fig. 12 Zoomed view of line current for different CC scheme.

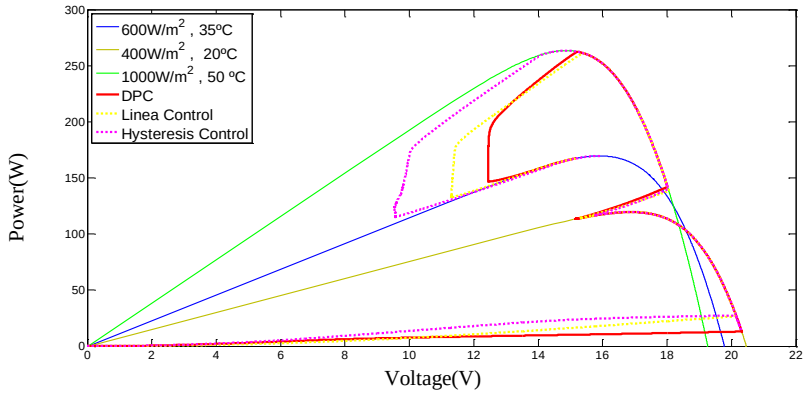

Fig. 13 Operational point of PV-array through MPPT under varying environmental

conditions

The result of FFT analysis done on line currents and number of switching for different CC schemes are summarised in Table 3.

Table 3 Line current THD and NO. of switching for different CC schemes.

	Line Current THD	Number of switching
Hysteresis Control	0.54%	13.24/cycle
Linear Control	5.65%	10.66/cycle
DPC	6.85%	12.39 /cycle

Fig. 13 shows operational point of PV-array through MPPT under varying environmental conditions for different CC schemes.

According to simulation results CC schemes are quite the same in terms of number of required switching, dynamic performance and MPPT performance, although they have just noticeable difference in injected current quality. Hysteresis control scheme can be pointed out as better scheme among CC schemes.

5. Conclusion

In This paper a simple structure for grid-connected PV system have been presented. The integration of PV system with grid is done by grid connected inverter. Three CC schemes including hysteresis CC, linear CC, and DPC have been presented for grid connected inverter to balance power flow between PV system and grid. The complete grid connected PV system have been simulated in MATLAB/Simulink® and results have been compared in terms of line current quality, dynamic performance, MPPT performance and number of required switching. Finally hysteresis CC pointed out as more suitable CC scheme duo to its better line current quality.

References

[1] Matsui, M., & Kitano, T.,& Xu, D.H., and Yang ,Z.Q. (1999). A New Maximum Photovoltaic Power Tracking Control Scheme Based on Power Equilibrium at DC Link . *Proceedings of the IEEE IAS Annual Meeting*, 804-809.

[2] Kitano,T. & . Matsui,M & Xu, D.-h.(2001) .Power sensor-less MPPT control scheme utilizing power balance at DC link-system design to ensure stability and response. *27th Annual Conference of the IEEE Industrial Electronics Society*,1309-1314.

[3] Esram,T.& Chapman,P.L.(2007).Comparison of Photovoltaic Array Maximum Power Point Tracking Techniques. *IEEE Trans. on Energy Conv.*, 22(2), 439-449.

[4] Liu, F. & Duan, S. & Liu, F. & Liu, B. & Kang, Y.(2008).A Variable Step Size INC MPPT Method for PV Systems. *IEEE Trans. Ind. Electron.*, 55(7) ,2622–2628.

[5] Zhao, R. & Chang, Z. & Yuan,P. & Yang, L. & Li, Z.(2009) .A Novel Fuzzy Logic and Anti-windup PI Controller for Three-phase Grid Connected Inverter. *2nd Int. Conf. on Power Electronics and Intelligent Transportation System*.

[6] Trzynadlowski, A. M.(1998) .Introduction to Modern Power Electronics" John Wiley & Sons, 318-319.

[7] Noguchi, T. & Tomiki, H. & Kondo, S. & Takahashi, I.,(1998) .Direct Power Control Of PWM Converter Without Power Source Voltage Sensors. *IEEE Trans. Ind. Applications*. 34(3),473–479.

[8] Baktash, A. & Vahedi, A. & S. Masoum, M.A. (2009) .New Switching Table For Improved Direct Power Control Of Three-Phase PWM Rectifier. *Australian Journal of Electrical & Electronics Engineering*, 5(2).

[9] Walker,G. (2001).Evaluating MPPT Converter Topologies Using A MATLAB PV Model. *Journal of Electrical & ElectronicsEngineering*. 21(1),49-56.